

Structural Phase Transitions of ZnTe under High Pressure Using Experiments and Calculations *

Hu Cheng(程虎)^{1,2}, Yan-Chun Li(李延春)^{2**}, Gong Li(李工)¹, Xiao-Dong Li(李晓东)²

¹State Key Laboratory of Metastable Materials Science and Technology, Yanshan University, Qinhuangdao 066004

²Beijing Synchrotron Radiation Facility, Institute of High Energy Physics, Chinese Academy of Sciences, Beijing 100049

(Received 2 June 2016)

The pressure-induced structural transitions of ZnTe are investigated at pressures up to 59.2 GPa in a diamond anvil cell by using synchrotron powder x-ray diffraction method. A phase transition from the initial zinc blende (ZB, ZnTe-I) structure to a cinnabar phase (ZnTe-II) is observed at 9.6 GPa, followed by a high pressure orthorhombic phase (ZnTe-III) with *Cmcm* symmetry at 12.1 GPa. The ZB, cinnabar (space group $P3_121$), *Cmcm*, $P3_1$ and rock salt structures of ZnTe are investigated by using density functional theory calculations. Based on the experiments and calculations, the ZnTe-II phase is determined to have a cinnabar structure rather than a $P3_1$ symmetry.

PACS: 61.50.-f, 61.50.Ks, 81.30.Hd

DOI: 10.1088/0256-307X/33/9/096104

In the last few decades, the structural and electronic behaviors of ZnX ($X=O, S, Se$ and Te) have been extensively investigated due to their outstanding optical properties, such as visual displays, high density optical memories, transparent conductors, solid-state laser devices, photodetectors and solar cells.^[1] However, the high pressure structures of ZnTe are a point of the ongoing debate. Experiments and calculations show that ZnTe exhibits more complicated structural behaviors under pressures than the other zinc chalcogenides (ZnS and ZnSe), which transform directly from zinc blende (ZB) or wurtzite to rock salt (RS) structure,^[2–5] and the other tellurides (CdTe and HgTe), which transform from ZB to the cinnabar structure and then to RS structure.^[6,7]

Samara *et al.* found that there were three sharp changes in electrical resistivity for ZnTe below 15 GPa.^[8] However, diffraction experiments showed that only two of the resistivity changes observed by Samara *et al.* correspond to structural phase transitions.^[2] Combined x-ray-diffraction and electric resistivity measurements, Ohtani *et al.* found that there are two structural transitions at approximately 8.5 GPa (to nonmetallic ZnTe-II) and 13.0 GPa (to metallic ZnTe-III).^[9] However, their x-ray diffraction data are insufficient to determine the high pressure structures. Subsequently, a combination of x-ray-absorption spectroscopy and x-ray diffraction studies showed that the crystallographic transition pressures are 9.5 ± 0.5 and 12 ± 0.5 GPa, and proposed the cinnabar structure for ZnTe-II.^[10] Nelmes *et al.* confirmed the cinnabar structure for the ZnTe-II phase and determined the ZnTe-III phase as the orthorhombic structure with *Cmcm* symmetry using angle-dispersive powder-diffraction techniques with an image-plate area-detector and synchrotron radiation.^[11–13] However, Kusaba *et al.* pro-

posed a space group $P3_1$ rather than $P3_121$ for ZnTe-II at 11.5 GPa based on the energy dispersive x-ray powder diffraction patterns.^[14] With the advances in ab initio methods, it has become possible to compute the structural,^[15–20] mechanical,^[20–22] electronic^[18–21,23] and optical properties^[18,19,21,23] of ZnTe with a great accuracy. Therefore, numerous studies aiming to develop microscopic understanding of pressure induced phase behavior of ZnTe have been performed in the past few decades. Despite the growing interest in the physical properties of ZnTe at high pressure, the structure of the ZnTe-II phase is always controversial. The persuasive compression behaviors of the two high-pressure phases of ZnTe have been unavailable.

In this Letter, the phase transitions of ZnTe are investigated using the synchrotron x-ray diffraction method (XRD) at pressures up to 59 GPa under hydrostatic conditions. The hydrostatic environment is useful for obtaining high-resolution diffraction patterns. The phase transition from the ZB to the cinnabar phase is observed above 9.6 Pa, followed by another phase transition to the *Cmcm* phase at 12.1 GPa, which is in agreement with previous reports. Based on our results, it is believed that the ZnTe-II phase actually possesses a cinnabar symmetry, rather than a $P3_1$ structure. In addition, refined patterns of the three phases are obtained. The results are confirmed by density functional theory (DFT) calculations. Moreover, we derive the equation-of-state (EOS) parameters of the high-pressure phase of ZnTe.

High-pressure experiments were performed in a symmetric diamond anvil cell (DAC) with a pair of diamond anvils with a culet diameter of 300 μm . The sample was ground into powder, pressed into a thin slice, and then placed in a 150- μm -diameter hole in a pre-indented stainless steel gasket with 40 μm

*Supported by the National Natural Science Foundation of China under Grant No 11474280, the National Basic Research Program of China under Grant No 2011CB808200, and the Chinese Academy of Sciences under Grant Nos KJ CX2-SW-N20 and KJ CX2-SW-N03.

**Corresponding author. Email: liyc@ihep.ac.cn

© 2016 Chinese Physical Society and IOP Publishing Ltd

thickness. Ne served as the pressure transmitting medium to provide the quasi-hydrostatic environment in our experiment using a BSRF-4W2 compressed gas loading system up to 59.2 GPa. In the experiment, ruby chips were used for the pressure calibration by measuring the fluorescence shift as a function of pressures.^[24] In situ high-pressure XRD experiments were conducted at the 4W2 beamline of the Beijing Synchrotron Radiation Facility (BSRF) using the angle-dispersive diffraction method with the beam wavelength of 0.6199 Å. An x-ray beam was focused in the horizontal and vertical directions to a $34 \times 13 \mu\text{m}^2$ spot by using Kirkpatrick-Baez mirrors. The powder diffraction patterns were collected with a Pilatus image plate and integrated with the FIT2D software package.^[25] The diffraction data were then analyzed by using the GSAS program.^[26]

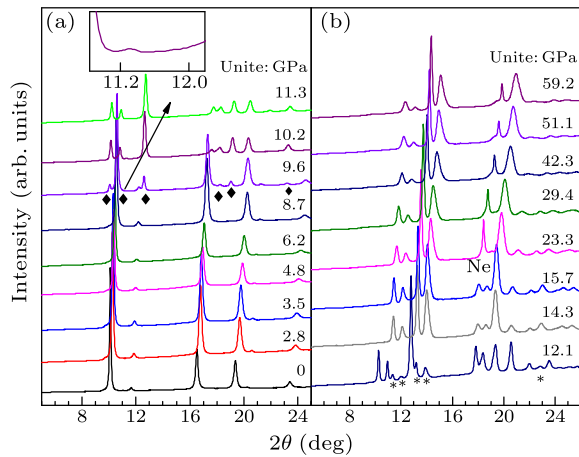


Fig. 1. The x-ray diffraction patterns of ZnTe plotted against pressure with Ne as the pressure transmitting medium.

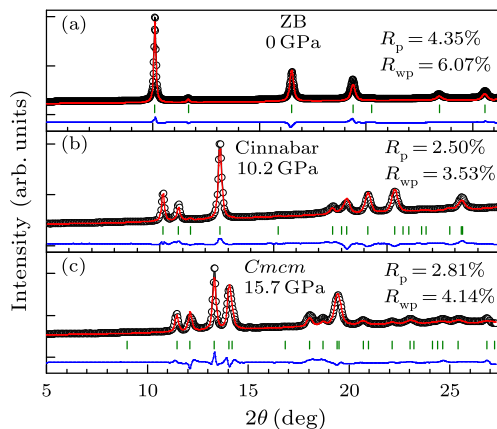


Fig. 2. Rietveld refinement patterns of the ZB, cinnabar, and *Cmcm* phases of ZnTe. (a) Rietveld refinement pattern of the ZB phase under ambient conditions. (b) Rietveld refinement pattern of the cinnabar phase at 10.2 GPa. (c) Rietveld refinement pattern of the *Cmcm* phase at 15.7 GPa.

DFT calculations were performed by using the plane-wave method with ultra-soft pseudopotentials.^[27] Here we used the generalized

gradient approximation (GGA)^[28] and local density approximation (LDA)^[29] to calculate the exchange and correlation energies. All structural optimizations under high pressures were performed with the Broyden–Fletcher Goldfarb–Shanno algorithm.^[30]

The crystal structures examined for the ZnTe here are as follows: (1) In the ZB structure ($F-43m$), the Zn atom is at the position of (0, 0, 0) and the Te atom is at the position of (0.25, 0.25, 0.25) in the primitive unit cell; (2) cinnabar structure ($P3_121$), the Zn atom is at the position of (0.542, 0, 0.3333) while the Te atom is at the position of (0.506, 0, 0.8333)^[12] in the primitive unit cell; (3) in the RS structure ($Fm3m$), the Zn atom is at the position of (0, 0, 0) and the Te atom is located at the position of (0.5, 0.5, 0.5) in the primitive unit cell;^[31] (4) for *Cmcm*, the Zn atom is at the position of (0, 0.640, 0.25) and the Te atom is located at the position of (0, 0.190, 0.25)^[11] in the primitive unit cell; and (5) for $P3_1$, the Zn atom is at the position of (0.35, 0.2, 0) and the Te atom is located at the position of (0.49, 0.49, 0.47)^[14] in the primitive unit cell.

The cut-off energy was set to 1000 eV and the k points were set to $4 \times 4 \times 4$ for the ZB phase, $4 \times 4 \times 2$ for the cinnabar phase, $5 \times 4 \times 5$ for the *Cmcm* phase, $4 \times 4 \times 4$ for the RS phase, and $4 \times 4 \times 2$ for the $P3_1$ phase. Convergence conditions were set to ultra-fine and the pressure ranges were set to 0–50 GPa in intervals of 5 GPa.

Figure 1 shows the diffraction patterns of ZnTe at various pressures with Ne as the pressure transmitting medium. The standard diffraction pattern of the ZB phase is shown at 0 GPa in Fig. 1(a). There are six diffraction peaks observed for the ZB phase of ZnTe. Figure 2(a) shows the Rietveld refinement pattern of the ZB phase at 0 GPa from which we obtain the lattice parameter $a = 6.1056(1)$ Å. The ZB phase of ZnTe is stable up to 8.7 GPa in Fig. 1(a). At ~ 9.6 GPa, the appearance of six new diffraction peaks (denoted with black rhombus) indicates the onset of the first phase transition. Upon further compression, the phase is stable up to about 12 GPa, which is in agreement with the previous reports.^[9–11,31,33–37] When the pressure reaches 12.1 GPa, five new diffraction peaks (denoted with asterisks) can be observed in Fig. 1(b), which indicates another phase transition. The new high-pressure phase is stable up to at least 59.2 GPa. The diffraction patterns at 10.2 GPa and 15.7 GPa in the experiment have been indexed into a cinnabar structure and an orthorhombic structure with a *Cmcm* space group, respectively. The diffraction patterns have been refined by using the Rietveld method in the GSAS program. Figure 2 shows the Rietveld refinement patterns of the three phases of ZnTe: the ZB, cinnabar and *Cmcm* phases. The lattice parameters for the cinnabar structure are $a = b = 4.054(2)$ Å, and $c = 9.425(4)$ Å at 10.2 GPa, and that of the *Cmcm* phase is $a = 5.339(4)$ Å, $b = 5.869(2)$ Å, and $c = 5.016(1)$ Å at 15.7 GPa, and these are consistent

with those obtained by Nelmes *et al.*^[11–13]

However, the ZnTe-II phase between the ZB and *Cmcm* phases for ZnTe is controversial in different studies.^[11–14] To confirm the structure of the ZnTe-II phase, the calculated patterns of the cinnabar and $P3_1$ structures of ZnTe and the experimental patterns are compared in the present study. Furthermore, we give the calculated pattern of the SC16 phase, which is suggested to be more stable than the cinnabar phase by Biering *et al.*^[32] through calculation. Figure 3 shows the calculated patterns of the cinnabar (Fig. 3(b)), $P3_1$ (Fig. 3(c)), SC16 (Fig. 3(d)) structures and the diffraction patterns of the ZnTe-II phase in our experiment (Fig. 3(a)). As shown in Fig. 3, the calculated pattern of the SC16 structure is completely different from the experimental pattern in two aspects of the intensity and positions of diffraction peaks. The calculated pattern of the $P3_1$ phase is slightly similar to the experimental pattern, while the intensity of some reflections (denoted with asterisk) are quite different from those of the experimental patterns. Contrary to SC16 and $P3_1$ structures, the calculated pattern of the cinnabar phase is more consistent with the experiments. This indicates that the ZnTe-II phase does not possess the $P3_1$ structure, while it has a cinnabar structure.

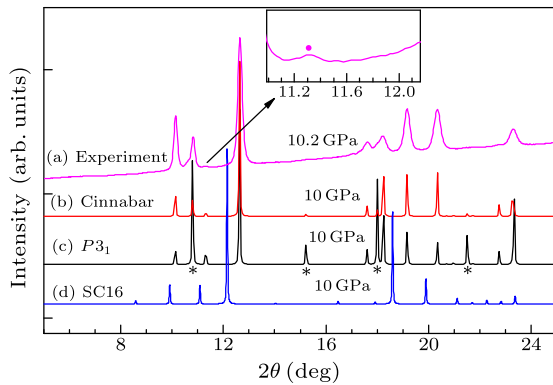


Fig. 3. Diffraction pattern of ZnTe in the present experiment (a). Calculated patterns of the cinnabar (b), $P3_1$ (c) and SC16 (d) structures of ZnTe.

To confirm the results of the experiments, the relationships between the energy and volume (E - V) are calculated for five structures, i.e., the ZB, cinnabar, $P3_1$, *Cmcm*, and RS phases, by using the GGA (Fig. 4(a)) and the LDA (Fig. 4(b)). The stable phase for a given volume is the one with the lowest total energy in terms of the thermodynamic stability. As shown in Fig. 4, the initial stable phase of ZnTe is the ZB phase. With decreasing the volume, the ZB phase becomes unstable and a transition from the ZB to cinnabar phase occurs. The ZnTe-II phase between the ZB and *Cmcm* phases of ZnTe has been proposed for some time by Nelmes *et al.*^[11–13] and Kusaba *et al.*^[14] respectively. However, there is no comprehensive comparison between the cinnabar and $P3_1$ phases. Through our calculations shown in Fig. 4, it can be

found that the cinnabar phase has the lowest energy in the five structures in the volume ranges of 41–45.5 Å³ (Fig. 4(a)) and 45–47.5 Å³ (Fig. 4(b)). This is consistent with the previously experimental and computational results. With further decreasing volume, the energy of the *Cmcm* phase drops to the lowest, and it has a stable structure. Over the whole pressure range, the RS form does not occur in the transition process of ZnTe according to our calculations and experiments. In conclusion, calculated results are consistent with our experimental crystal structural transformation sequence of ZB to cinnabar to *Cmcm*.

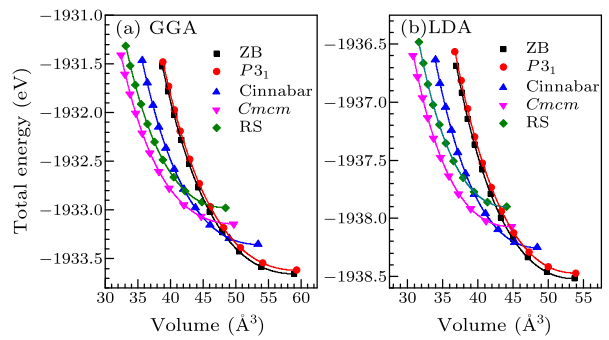


Fig. 4. Calculated total energy versus volume for the ZB, cinnabar, $P3_1$, *Cmcm*, and RS phases of ZnTe. (a) Using the GGA and (b) using the LDA.

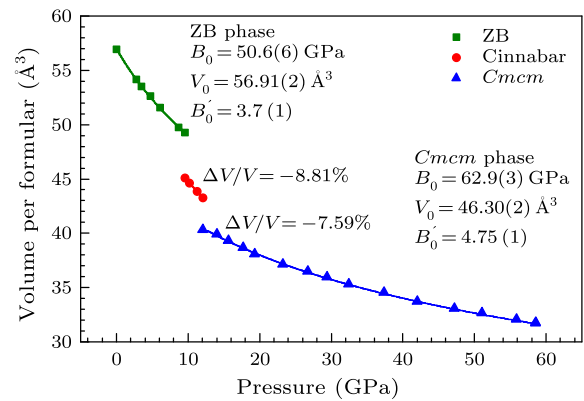


Fig. 5. Unit cell volume of the ZB, cinnabar, and *Cmcm* phases of ZnTe plotted against pressure.

The pressure-volume (P - V) relationships of the ZB, cinnabar, and *Cmcm* phases are shown in Fig. 5. The changes in volume from the ZB to cinnabar and cinnabar to *Cmcm* phases are 8.81% and 7.59%, respectively. These P - V data were fitted into the third-order Birch-Murnaghan equation of state to obtain the bulk modulus B_0 and its pressure derivative B'_0 of each phase of ZnTe. Table 1 summarizes the equilibrium volumes V_0 , bulk modulus B_0 , and pressure derivatives, under different experimental conditions. The experimental B_0 of the ZB phase ($B_0 = 50.6(6)$ GPa with $V_0 = 56.91(2)$ Å³ and $B'_0 = 3.7(1)$) is consistent with previously reported results^[10,35,38–40] and our calculated results using the GGA ($B_0 = 44.8(7)$ GPa with $V_0 = 59.04(8)$ Å³ and $B'_0 = 4.57(4)$) and LDA ($B_0 = 56.7(2)$ GPa with $V_0 = 53.64(1)$ Å³

and $B'_0 = 4.57(1)$), while are much smaller than the experimental values obtained by Onodera *et al.* ($B_0 = 76.4$ GPa with $B'_0 = 3.0$).^[31] Unfortunately, due to the very narrow existing pressure range of the

cinnabar phase, only two pressure points, at which the cinnabar phase is dominated, have been obtained and cannot be fitted to the equation of state.

Table 1. Equilibrium volume V_0 , volume modulus B_0 , its pressure derivative B'_0 and phase transition pressures in different experiments and calculations.

	ZnTe-I			ZnTe-II			ZnTe-III			References
	V_0 (\AA^3)	B_0 (GPa)	B'_0	V_0 (\AA^3)	B_0 (GPa)	B'_0	V_0 (\AA^3)	B_0 (GPa)	B'_0	
Experiment										
	56.91(2)	50.6(6)	3.7(1)				46.30(2)	62.9(3)	4.75(1)	Present
		50.5	5							[10]
		51(3)	3.6(0.8)							[35]
		76.4	3.0		91.3	0.8		134	2.4	[31]
		50.8(7)	5.08							[38]
		48.0	4.7							[39]
		48.8	3.7							[40]
Calculation										
	59.04(8)	44.8(7)	4.57(4)	53.47(4)	47.6(4)	4.66(2)	48.8(2)	44.9(9)	4.8(1)	Present (GGA)
	53.64(1)	56.7(2)	4.57(1)	48.46(1)	61.8(2)	4.60(1)	44.47(3)	60.2(6)	4.78(5)	Present (LDA)
	58.39	47.7	4.7	52.96	51.4	4.5	46.75	62.2	4.7	[17]
	58.73	45.25	4.26	52.66	49.70	4.45	47.74	58.79	5.09	[18]
		55.21	4.60							[21]
		41.6	4.87		46.68	4.69		54.07	4.7	[22]
		44.35								[43]

The bulk modulus B_0 of the *Cmcm* phase of ZnTe in our experiment ($B_0 = 62.9(3)$ GPa with $V_0 = 46.30(2) \text{\AA}^3$ and $B'_0 = 4.75(1)$) is in agreement with our calculated results by using the LDA ($B_0 = 60.2(6)$ GPa with $V_0 = 44.47(3) \text{\AA}^3$ and $B'_0 = 4.78(5)$) and the results in Ref. [17] ($B_0 = 62.2$ GPa with $V_0 = 46.75 \text{\AA}^3$ and $B'_0 = 4.7$). However, the bulk modulus B_0 of the *Cmcm* phase of our calculated results by using the GGA and LDA are smaller than those of the cinnabar phase calculated by using the GGA ($B_0 = 47.6(4)$ GPa with $V_0 = 53.47(4) \text{\AA}^3$ and $B'_0 = 4.66(2)$) and the LDA ($B_0 = 61.8(2)$ GPa with $V_0 = 48.46(1) \text{\AA}^3$ and $B'_0 = 4.60(1)$), and are different from the previously works,^[17,18,22] where the bulk modulus B_0 of the *Cmcm* phase are obviously larger than those of the cinnabar phase. We consider that the *Cmcm* phase of ZnTe as a metal phase which have proved by electrical resistance measurements^[8,9,44] is more compressible than the semi-conductive cinnabar phase.

In summary, based on synchrotron XRD and DFT calculations, the phase transitions of ZnTe have been investigated under high pressure. In high-pressure experiments, a phase transition from the ZB to the cinnabar phases was observed at 9.6 GPa, followed by another phase transition from the cinnabar to *Cmcm* phases at 12.1 GPa, which is consistent with previously published results. Especially, some candidates of the ZnTe-II phase, such as the cinnabar and $P3_1$ symmetry and SC16 structures, have been compared in detail, and we confirm that the ZnTe-II phase has a cinnabar structure. The diffraction patterns of the three phases have been refined by using the Rietveld method in the GSAS program. The relationships of

energy versus volume and enthalpy versus pressure of the ZB, cinnabar, $P3_1$, RS and *Cmcm* phases were investigated by DFT calculations, and the results confirmed the results of the experiments.

References

- [1] Karazhanov Zh S, Ravindran P, Kjekshus A, Fjellvåg H and Svensson B G 2007 *Phys. Rev. B* **75** 155104
- [2] Smith P L and Martin J E 1965 *Phys. Lett.* **19** 541
- [3] Ves S, Schwarz U, Christensen N E, Syassen K and Cardona M 1990 *Phys. Rev. B* **42** 9113
- [4] Bilge M, Kart S O, Kart H H and Cagin T 2008 *Mater. Chem. Phys.* **111** 559
- [5] Kalay M, Kart H H, Kart S O and Cagin T 2009 *J. Alloys Compd.* **484** 431
- [6] McMahon M I, Nelmès R J, Wright N G and Allan 1993 *Phys. Rev. B* **48** 16246
- [7] Werner A, Hochheimer H D, Strössner K and Jayaraman D R A 1983 *Phys. Rev. B* **28** 3330
- [8] Samara G A and Drickamer H G 1962 *J. Phys. Chem. Solids* **23** 457
- [9] Ohtani A, Motobayashi M and Onodera A 1980 *Phys. Lett. A* **75** 435
- [10] Miguel A S, Polian A and Ganthier M 1993 *Phys. Rev. B* **48** 8683
- [11] Nelmès R J, McMahon M I, Wright N G and Allan D R 1994 *Phys. Rev. Lett.* **73** 1805
- [12] McMahon M I, Nelmès R J, Wright N G and Allan D R 1994 *In Proc. of the Joint AIEAPTAPS Topical Conf. on High Pressure Science and Technology* edited by Schmidt S C, Shoner J W, Samara G A and Ross M (New York: American Institute of Physics)
- [13] Nelmès R J, McMahon M I, Wright N G and Allan D R 1995 *J. Phys. Chem. Solids* **56** 545
- [14] Kusaba K and Donald J W 1994 *AIP Conf. Proc.* **309** 553
- [15] Côté M, Zakharov M, Rubio A and Cohen M L 1997 *Phys. Rev. B* **55** 13025
- [16] Lee G D, Hwang C, Lee M H and Ihm J 1997 *J. Phys.: Condens. Matter* **9** 6619
- [17] Franco R, Mori-Sanchez P, Recio J M and Pandey R 2003

- Phys. Rev. B* **68** 195208
- [18] Gupta S K, Kumar S and Auluck S 2009 *Physica B* **404** 3789
- [19] Nourbakhsh Z 2010 *J. Alloys Compd.* **505** 698
- [20] Agrawal B K, Yadav P S and Agrawal S 1994 *Phys. Rev. B* **50** 14881
- [21] Khenata R, Bouhemadou A, Sahnoun M, Reshak A H, Baltache H and Rabah M 2006 *Comput. Mater. Sci.* **38** 29
- [22] Soykan C and Kart S O 2012 *J. Alloys Compd.* **529** 148
- [23] Merad A E, Kanoun M B, Merad G, Cibert J and Aourag H 2005 *Mater. Chem. Phys.* **92** 333
- [24] Mao H K, Xu J and Bell P M 1986 *J. Geophys. Res.* **91** 4673
- [25] Hammersley J 1996 *Fit2d User Manual* (Grenoble: ESRF)
- [26] Toby B H 2001 *J. Appl. Crystallogr.* **34** 210
- [27] Troullier N and Martins J L 1991 *Phys. Rev. B* **43** 1993
- [28] Perdew J P and Yue W 1986 *Phys. Rev. B* **33** 8800
- [29] Hedin L and Lundqvist B I 1971 *J. Phys. C* **4** 2064
- [30] Pfrommer B G, Cote M, Louie S G and Cohen M L 1997 *J. Comput. Phys.* **131** 233
- [31] Onodera A, Ohtani A, Tsuduki S and Shimomura O 2008 *Solid State Commun.* **145** 374
- [32] Biering S and Schwerdtfeger P 2012 *J. Chem. Phys.* **137** 034705
- [33] Endo S, Yoneda A and Ishikawa M 1982 *J. Phys. Soc. Jpn.* **51** 38
- [34] Strossner K, Ves S, Kim C K and Cardona M 1987 *Solid State Commun.* **61** 275
- [35] Kusaba K, Galois L, Wang Y, Vaughan M T and Weidner D J 1993 *PAGEOPH* **141** 643
- [36] Qadri S B, Skelton E F, Webb A W, Hu J Z, Schmidt S C, Shaner J W, Samara G A and Ross M 1994 *High Pressure Science and Technology-1993* (New York: AIP Press) p 319
- [37] Shimomura O, Utsumi W, Urakawa T, Kikegawa T, Kusaba K and Onodera A 1997 *Rev. High Press. Sci. Technol. (Spec. Issue)* **6** 207
- [38] Lee B H 1970 *J. Appl. Phys.* **41** 2988
- [39] Strössner K, Ves S, Kim C K and Cardona M 1987 *Solid State Commun.* **61** 275
- [40] Shimomura O, Utsumi W, Urakawa S, Yamakata M, Kikegawa T and Onodera A 1992 *Proc. 33rd High Pressure Conf.* (in Japan) p 464
- [41] Lee G, Lee M H and Ihm J 1995 *Phys. Rev. B* **52** 1459
- [42] Gangadharan R, Jayalakshmi V, Kalaiselvi J, Mohan S, Murugan R and Palanivel B 2003 *J. Alloys Compd.* **359** 22
- [43] Charifi Z, Hassan F E H, Baaziz H, Khosravizadeh S, Hashemifar S J and Akbarzadeh H 2005 *J. Phys.: Condens. Matter* **17** 7077
- [44] Ovsyannikov S V and Shchennikov V V 2004 *Solid State Commun.* **132** 333